

# GripAble: An accurate, sensitive and robust digital device for measuring grip strength

Journal of Rehabilitation and Assistive Technologies Engineering  
Volume 9: 1–12  
© The Author(s) 2022  
Article reuse guidelines:  
[sagepub.com/journals-permissions](https://sagepub.com/journals-permissions)  
DOI: 10.1177/20556683221078455  
[journals.sagepub.com/home/jrt](https://journals.sagepub.com/home/jrt)  


Michael Mace<sup>1,\*</sup> , Sarah Abdul Mutalib<sup>1,2,\*</sup> , Matjaz Ogrinc<sup>1,2</sup> , Nicola Goldsmith<sup>1,3</sup> and Etienne Burdet<sup>2</sup>

## Abstract

**Introduction:** Grip strength is a reliable biomarker of overall health and physiological well-being. It is widely used in clinical practice as an outcome measure. This paper demonstrates the measurement characteristics of GripAble, a wireless mobile handgrip device that measures grip force both isometrically and elastically-resisted for assessment and training of hand function.

**Methods:** A series of bench tests were performed to evaluate GripAble's grip force measurement accuracy and sensitivity. Measurement robustness was evaluated through repeated drop tests interwoven with error verification test phases.

**Results:** GripAble's absolute measurement error at the central position was under 0.81 and 1.67 kg (95<sup>th</sup> percentiles; N = 47) when measuring elastically and isometrically, respectively, providing similar or better accuracy than the industry-standard Jamar device. Sensitivity was measured as  $0.062 \pm 0.015$  kg (mean  $\pm$  std; 95<sup>th</sup> percentiles: [0.036, 0.089] kg; N = 47), independent of the applied force. There was no significant performance degradation following impact from 30 drops from a height >1.5 m.

**Conclusion:** GripAble is an accurate and reliable grip strength dynamometer. It is highly sensitive and robust, which in combination with other novel features (e.g. portability, telerehabilitation and digital data tracking) enable broad applicability in a range of clinical caseloads and environments.

## Keywords

Grip strength, dynamometry, hand therapy, occupational therapy, physiotherapy, force sensing, assessment, neurorehabilitation, telerehabilitation, home-based rehabilitation, GripAble, Jamar

Date received: 2 August 2021; accepted: 20 January 2022

## Background

*Grip strength* is understood to be a reliable biomarker of overall health and physiological well-being, including ageing, disability, morbidity and mortality, in elderly,<sup>1</sup> middle-aged<sup>2</sup> and younger adults.<sup>3</sup> The measurement of *maximal hand grip strength* is increasingly used for evaluating muscle strength<sup>4</sup> and muscle mass,<sup>5</sup> diagnosing the extent of neurological impairments and injury, and monitoring motor learning and recovery post-rehabilitation.<sup>6,7</sup>

<sup>1</sup>GripAble Limited, London, UK

<sup>2</sup>Bioengineering Department, Imperial College of Science Technology and Medicine, London, UK

<sup>3</sup>NES Hand Therapy Training, London, UK

\*These authors contributed equally to this work.

Corresponding author:

Sarah Abdul Mutalib, GripAble Limited, London, UK.

Email: [sharah@gripable.co](mailto:sharah@gripable.co)



Creative Commons Non Commercial CC BY-NC: This article is distributed under the terms of the Creative Commons Attribution-NonCommercial 4.0 License (<https://creativecommons.org/licenses/by-nc/4.0/>) which permits non-commercial use, reproduction and distribution of the work without further permission provided the original work is attributed as specified on the

SAGE and Open Access pages (<https://us.sagepub.com/en-us/nam/open-access-at-sage>).

Grip strength has also been used to stratify an individual's future risk to health problems, such as cardiovascular mortality and frailty due to sarcopenia.<sup>5</sup> For example, a 5 kg decline in grip strength over a 4-year period is associated with a 17%, 7% and 9% increased risk of cardiovascular death, heart attack and stroke, respectively.<sup>8</sup>

Grip strength is measured quantitatively using a hand dynamometer. The *Jamar* (J.A. Preston Corporation, Clifton, NJ) hand dynamometer is the industry-standard device for measuring maximal hand grip strength<sup>9</sup> developed in 1954 by Bechtol.<sup>10</sup> *Jamar* was first popularised by Mathiowetz in 1985<sup>11</sup> and is currently recommended by the American Society of Hand Therapists.<sup>12,13</sup> When used according to standard positionings and instructions,<sup>12,13</sup> a properly calibrated *Jamar* is accurate, reliable and has good-to-excellent test-retest reliability ( $p = 0.88\text{--}0.93$ ) and excellent interrater reliability ( $p = 0.99$ ).<sup>14</sup> There are also many replicas of *Jamar*, such as *Baseline*,<sup>15</sup> *Rolyan*<sup>9</sup> (discontinued) and *GripTrack*<sup>16</sup> (discontinued), offering similar design and functionality. Nevertheless, *Jamar* remains the gold-standard, despite having questionable robustness, is relatively heavy at 0.7 kg, relies on regular recalibration and has low resolution with readout measurement intervals of 2 kg. It also has poor sensitivity at the lower end of force, where it requires an initial force of 1.5–2 kg to move the needle,<sup>17</sup> which may be unsuitable for measuring grip strength in very weak individuals.

The primary reason for *Jamar*'s continued use is because it is the instrument used in Mathiowetz et al.'s normative grip strength studies on adults<sup>11</sup> and children,<sup>18</sup> which are most widely referred to by clinicians worldwide to compare a patient's grip strength to the healthy population – despite many new normative datasets published since. However, recent studies found that hand grip strength has weakened dramatically since 1985,<sup>19</sup> potentially due to anthropometric and lifestyle changes over the past 40 years. This finding, questions the validity of existing normative datasets, thus compromising the accuracy of today's clinical assessments. Therefore, a new dataset is required to understand what constitutes normal hand grip strength, which gives an opportunity to modernise the current industry standard.

The increasing use of maximal hand grip strength measures invoked many new hand dynamometers, claiming a broad spectrum of measurement performance. Many of them show good-to-excellent agreement to the industry-standard *Jamar*. However, as revealed in Table 1, many still lack proof of, or have never been bench tested to demonstrate, sufficient robustness and sensitivity – which are vital but often overlooked characteristics of an assessment device. A hand dynamometer is heavily used during rehabilitation. Therefore, the device should be robust enough to withstand accidental drops and maintain its optimal performance to ensure the validity of grip strength assessment. Meanwhile, a sensitive

assessment device is required for detecting grip strength changes, for example, in weak individuals such as post-stroke or post-surgery, who can often exhibit grip strength below 1 kg.

A reliable assessment device is important not only to enable clinicians to determine the need and efficacy of rehabilitation or surgery, but also to support a shift to remote care. Clinically used grip measurement devices should address such shifts by leveraging evolving mobile and digital health technology. Such advancement has the potential to improve multiple aspects of rehabilitation, including remote assessment and personalised training. A critical point has been reached whereby demand for remote *home-based rehabilitation*, or *telerehabilitation*, is at its peak, exacerbated by global pandemics, for example, COVID-19, causing the rehabilitation service for the majority of individuals to fall short.<sup>20–22</sup> Therefore, portable, and robust systems that can be used across hospital, clinic and home environments are needed to bridge the widening gap and enable assessment, engagement, and delivery of patient care outside of medical institutions.

Remote assessment and rehabilitation are not without their challenges. The protocol for measuring maximal hand grip strength, for example, requires a high level of standardisation to be considered valid, such as observing body posture, limb positions and the use of standardised instruction.<sup>12,13</sup> A digital device could automatically document and track these parameters while monitoring compliance to standardised protocols, for example, based on tracking device orientation and stability using auxiliary motion sensors. Moreover, the ability to allow clinicians to remotely analyse results, customise interventions, collaboratively set goals and monitor changes or improvements in grip strength over time will increase clinical utility.

The *GripAble handgrip device* is a multi-purpose portable device that incorporates force and motion sensors. It can monitor interaction and connect wirelessly to mobile devices, enabling the user to perform objective assessments of grip strength and wrist range-of-motion, monitor user's compliance to standard protocols such as tracking hand posture, and track user progress through a custom therapy app. According to Fess (1986), the two most crucial criteria of an assessment device are (1) reliability based on bench tests across multiple sessions and devices, and (2) high validity when compared against existing validated instruments. Fess further recommends (3) administrative instructions, (4) equipment criteria, (5) normative data, (6) instruction for interpretation and (7) a bibliography.<sup>23,24</sup> This paper aims to address the first point by investigating *GripAble*'s grip force measurement accuracy and sensitivity across multiple devices and sessions through a series of bench tests. Furthermore, the

key characteristic of robustness was also evaluated through repeated drop tests.

## Methods

### *GripAble: mobile grip strength assessment device*

Figure 1 shows the GripAble handgrip device and its dimensions. The device builds on previous research prototypes used in recent clinical and motor control studies.<sup>29,30</sup> Its accessibility has been demonstrated across a broad range of studies in individuals with upper-limb impairment, in contrast to conventional mobile interactions such as swiping, tapping and tilting.<sup>29</sup> It has also been used in a study on bimanual training in children with unilateral cerebral palsy from 7 to 15 years, encouraging interlimb synergies through visual coupling.<sup>31</sup>

The GripAble device weighs 240 g with dimensions as shown in Figures 1(b) and (c). The 48 mm front-to-back depth of the GripAble device was chosen to match the depth of the second smallest bar of the industry-standard Jamar dynamometer (i.e. 49 mm), which is the current

standardised position for testing grip strength.<sup>12,13</sup> The shape of the GripAble device was designed to conform to the shape of the first web space of the human hand. A gentle C-shaped curve allows for a good fit irrespective of adult hand size. It also ensures the device sits firmly and consistently in hand, thus minimising the impact of hand position on the accuracy of the measurements, as it encourages individuals to hold the device in a similar manner and position during each use.

The device incorporates a spring design with two load cells (2 x 50 kg flat wheatstone bridge strain gauge sensors; model SC700; manufacturer Sensor and Control Co. Ltd), alongside custom springs in a symmetric configuration<sup>32</sup> that enables single-axis 10 mm elastic deformation when squeezed, after which the force will be measured isometrically. This elastic structure is self-guiding without the need for friction-inducing guide rails, allowing all force to be transferred through the mechanism, ensuring sensitivity even at very low forces with accurate measurement across the full biomechanically valid range up to 90 kg (882.6 N). It also has a manual locking mechanism to allow the grip force to be measured either rigidly (i.e. isometric or locked

Table 1. Non-exhaustive list of available dynamometers that have been tested against the industry-standard Jamar. \*Values based on sensor datasheet rather than system testing; x = data not available.

Device	Accuracy	Sensitivity	Robustness	Equivalence with Jamar (Intraclass correlation coefficient, ICC)
Rolyan <sup>9</sup> (discontinued)	x	x	x	0.90 to 0.97
Grippit <sup>25</sup>	x	x	x	0.87 to 0.93
MyoGrip <sup>26</sup>	50 g *	10 g *	x	0.51 to 0.96
Takej <sup>27</sup>	x	x	x	0.90 to 0.95
Bodygrip <sup>28</sup>	x	x	x	0.93 to 0.95
GripTrack <sup>16</sup> (discontinued)	x	x	x	0.61 to 0.95

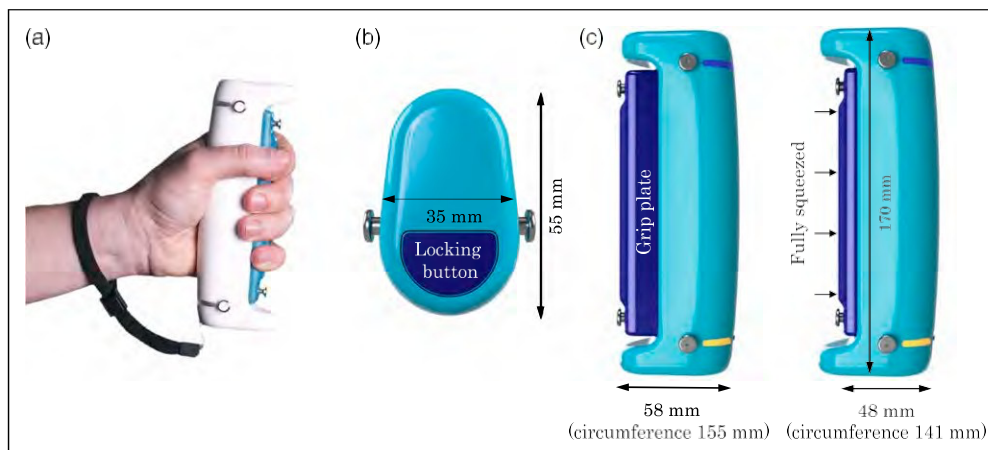


Figure 1. The GripAble handgrip device showing (a) the GripAble being grasped by an adult hand. (b) the width and breadth of the GripAble device from the top view. Also indicated is the locking button for switching between elastic (i.e. 'unlocked') and isometric (i.e. 'locked') modes. (c) The height of the GripAble device from the side view alongside the grip plate position in elastic (left) and isometric (right) modes.

mode) or against the springs (i.e. elastic or unlocked mode). The isometric mode allows GripAble to mimic existing rigid industry-standard dynamometers (e.g. Jamar) necessitated for grip strength measurements to be considered clinically valid. In the elastic mode, the device can be used for (concentric) grip and (eccentric) release training with the fingers' movement, acting to increase sensorimotor feedback and comfort. GripAble also incorporates embedded inertial motion sensors, for sensing device orientation, which can be used to infer wrist movements.

**Force measurement principle.** The grip force exerted onto the grip plate is transferred via parallel springs onto a fixed steel beam. Figure 2 shows the beam attached to the main body via two resistive beam load cells LC<sub>1</sub>, LC<sub>2</sub> with positions  $l_1$ ,  $l_2$  relative to the centre-of-pressure (CoP). The spring subsystem (shown simplified) has been designed to keep the grip plate and steel beam parallel during compression regardless of the position of the CoP within the (grey) region shown. After >10 mm of elastic deflection, the springs bottom out and the load is transferred directly into the steel beam. In this static condition, the grip plate and steel beam can be considered a single beam (under further compressive loads) with perpendicular forces and negligible beam deflection assumed.

In the static condition, the sum of all forces on the beam equals zero

$$\sum_i F_i = 0 \quad F = F_1 = F_2 \quad (1)$$

And the sum of moments about LC<sub>1</sub> is

$$\sum_i M_i = 0 \quad l_1 F = L F_2 \quad (2)$$

where  $L = l_1 + l_2$ . Forces  $F_1$ ,  $F_2$  can be estimated by measuring the electrical resistance  $r_1$ ,  $r_2$  of the load cells

$$F_1 = \frac{b_1}{k_1 r_1} = \frac{l_2}{L} F \quad (3)$$

$$F_2 = \frac{b_2}{k_2 r_2} = \frac{l_1}{L} F \quad (4)$$

when  $F$  is applied at a known location it can be inferred from either load cell reading, making this a redundant measurement system. Therefore, a combined estimate can be expressed as the average.

A calibration process is performed to identify the parameters  $b_1$ ,  $b_2$ ,  $k_1$ ,  $k_2$ , in which a sequence of reference forces ( $F$ ) are applied. Although temperature effects are well compensated by the Wheatstone bridge in each strain gauge, the biases can drift and vary over time due to changes in mechanical properties, for example, material fatigue from cyclic loading. Therefore, the zero drift is compensated in real-time by estimating the average force during periods of zero load when the device is untouched. An untouched state can be inferred based on the stability of the signal as the variation of the force signal will increase when touched due to physiological tremor. The estimated grip force is computed from

$$F = \frac{b_0}{k_1 r_1 + k_2 r_2} \quad (5)$$

$$b_0 = \frac{b_1}{k_1} + \frac{b_2}{k_2} + \epsilon_0 \quad (6)$$

where  $\epsilon_0$  is the zero-drift compensation term.

**Calibration.** The GripAble device is calibrated by collecting load cell voltages under known loads. Static loads are applied across the entire range of force of 0–90 kg (0–882.6 N), with an ordinary least squared (OLS) method used to identify calibration parameters ( $b_0$ ,  $k_1$ ,  $k_2$ ). Figure 3 shows an overview of the calibration setup and system block diagram. A force testing machine (Mecmesin MultiTest 2.5-i with ILC-1000 N load cell) provides ground truth loading (with accuracy < 100 g) while syncing with the GripAble load cell data captured over a serial interface (RS232) via a custom-

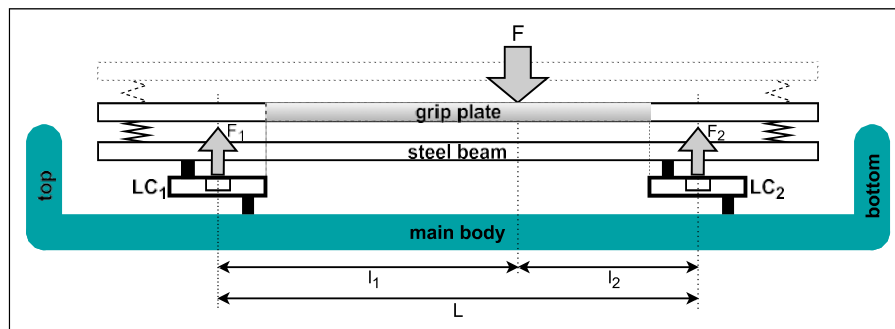


Figure 2. Schematic showing the spring subsystem and force measurement principle. The grip plate is shown in both elastic (i.e. springs extended - dotted outline) and isometric (i.e. springs compressed - solid outline) neutral positions. The load cells are short bending beams utilising wheatstone bridge strain gauges with the effective measurement positions (i.e. load cell midline) equidistant from the midline of the steel beam. The grey area shown on the grip plate indicates the region where  $F$  should be applied to keep the grip plate and steel beam parallel.

built calibration jig. The calibration process is controlled through a desktop computer running Mecmesin control software (Emperor) and a separate custom calibration application written in Python. A sync board is used to transmit sync events from the force testing machine to the calibration app and enables the data captured by the two systems to be synchronised offline. The custom calibration jig is used to secure the device in the correct orientation during the calibration process. It provides a temporary bi-directional RS232 interface for reading/writing data from/to the device. The load cell voltages are recorded in bits at 50 Hz, while the Mecmesin records data at 100 Hz. A 70 mm diameter calibration plunger, which is approximately the width of an adult human hand,<sup>35</sup> is used to exert a distributed contact force onto the grip plate. The calibration process and loading

requirements are based on the ISO 7500–1:2018<sup>33</sup> and ASTM E4-16:2016<sup>34</sup> standards, with the force testing machine annually recalibrated by the manufacturer.

The calibration process begins by placing the GripAble into the custom jig, enabling direct access to the serial communication interface located on the device’s printed circuit board. Once inserted, the custom automation software triggers a pre-programmed loading (compression) and unloading (relaxation) cycle. Figure 4(a) demonstrates the static compression phase up to 90 kg (882.6 N), in 10 kg (98.1 N) steps, followed by a similar relaxation phase, which together constitutes a single calibration trial. The software records 21 sync events triggered at the end of each static phase and enables the load cell voltages to be synchronised with the applied force measurements from the Mecmesin force testing machine by resampling all the data to 100 Hz and using cross-

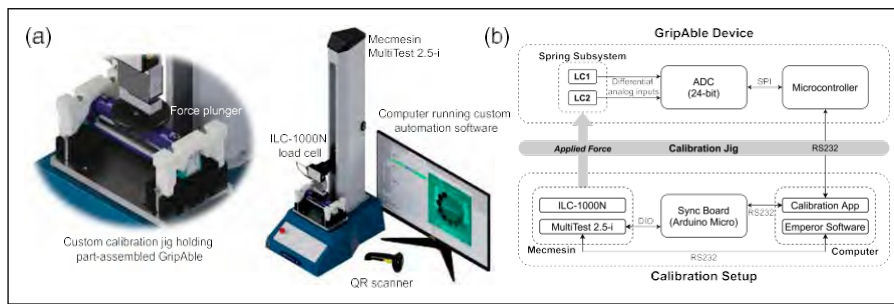


Figure 3. (a) Renderings of the factory calibration setup with key features annotated and (b) block diagram highlighting the key subcomponents and interfaces of the GripAble device and calibration setup in relation to the grip measurement function.

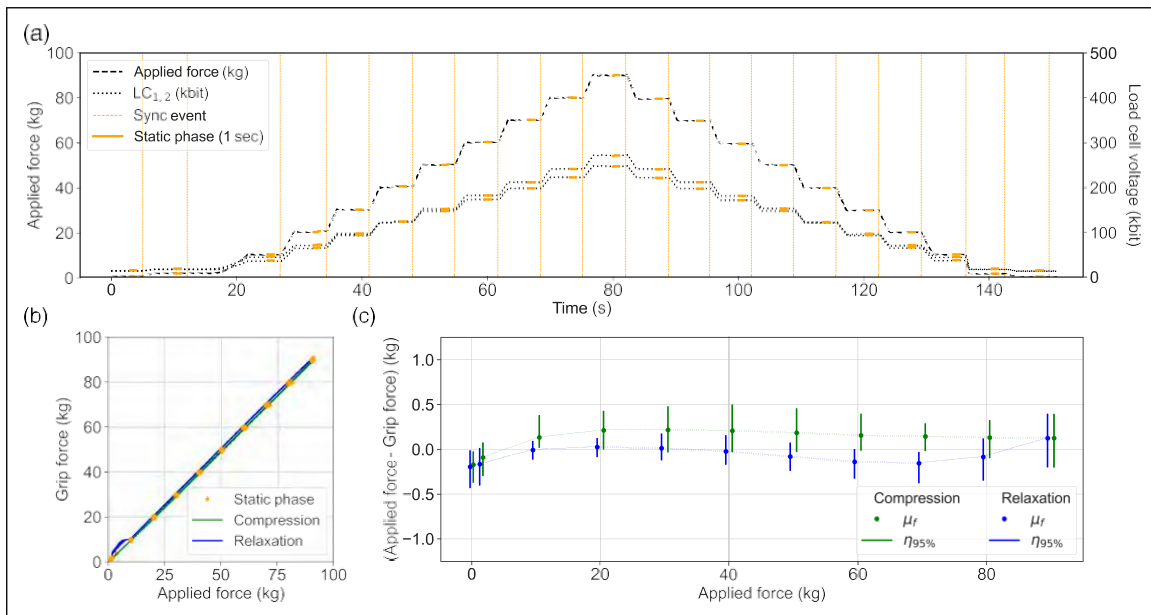


Figure 4. Calibration data and analysis. (a) Example raw data collected during a single grip force calibration trial, (b) grip force estimates against applied force for static and dynamic calibration phases for all 47 device trials and, (c) mean calibration errors and 95<sup>th</sup> percentiles at each static force level comparing the compression and relaxation phases.

correlation to align in the time domain. Static phases (1 second in duration) are extracted 1 second preceding the sync events for analysis. This provides 2–3 second for the Mecmesin machine to settle should there be any transients during the transfer to the hold phase. The applied force is generated by the Mecmesin force testing machine while the grip force is estimated from equation (5) using the raw load cell voltages and calibration parameters. The calibration app computes these calibration parameters based on the mean values during each static phase. They are then written to the GripAble device over the RS232 interface where they are stored in the embedded microcontroller's non-volatile random-access memory enabling the computed grip force estimate to be sent over Bluetooth post-calibration.

Figure 4(b) shows the estimated grip force overlaid for all 47 devices highlighting an excellent fit to the applied force  $R^2 = 0.9999$  for both the static and dynamic phases. A small kink at low forces during the dynamic relaxation phase is visible and can be attributed to the rapid transition from the isometric-to-elastic region (as opposed to the slow ramp up in the compression phase). Figure 4(c) shows the static training error distributions computed across the 47 devices for each static force level and loading direction (i.e. compression or relaxation) and highlights that the training error remains within  $\pm 0.5$  kg across all forces with a small hysteresis ( $< 0.4$  kg) between the compression and relaxation phases.

### Bench Tests

**Measurement accuracy against known loads.** Fess (1987) suggested measuring the *concurrent validity* and *error against known weights* to establish whether a device is accurate.<sup>36</sup> Therefore, a test was conducted to evaluate the measurement accuracy across multiple GripAbles ( $N = 47$ ) post-calibration. The two primary factors expected to affect measurement accuracy are the CoP of the hand relative to the grip plate and the measurement mode (i.e. elastic or isometric). Figure 5 shows a custom 3D printed tri-positional test jig holding the device in three positions (top, centre and bottom) relative to the force plunger. The centre position is in the same position as used during the calibration process. The top and bottom positions are equidistant from the centre position ( $\pm 13$  mm), representing the most extreme positions that the CoP of grip force could be applied when employing a cylindrical grasp.

The test jig was printed from PLA at 20% infill and exhibited no visible deformation when loaded at 90 kg (without the device) in all three positions. Each device was subjected to the same loading-unloading measurement cycle as performed in the calibration phase at each position (top, centre, bottom) and mode (elastic, isometric), making a total of six measurement cycles per device. Alternate test devices were mirrored relative to the midline of the calibration machine to ensure any positional errors between the device and plunger were averaged out.

The concurrent validity was measured from the Pearson correlation between the GripAble output and the applied (i.e. 'known') force.<sup>36</sup> Additionally, *hysteresis* was also calculated to evaluate whether the device's accuracy remains consistent during force compression and relaxation. The hysteresis was calculated for each trial by estimating two linear models for the loading and unloading cycles. The hysteresis was then obtained by calculating the maximum difference between the estimated force from these two linear models across the full measurement range of 0–90 kg (0–882.6 N), as a percentage of the full measurement range 90 kg (882.6 N).

**Measurement sensitivity.** GripAble's grip force measurement *sensitivity* was computed across 47 GripAbles. It was measured from the maximum peak-to-peak noise during the 1-second static loading phases as shown in Figure 4(a). A change in the grip force will only be detected if the signal changes by a value greater than this peak-to-peak noise.

**Drop robustness.** The impact from accidentally dropping a grip dynamometer could negatively influence the reliability of its measurement accuracy. During normal use, multiple drops are expected over the device's lifetime, for example, if the device is knocked from the table onto a hard surface. A drop test was conducted to understand the impact and effect of drops on measurement accuracy under worst-case conditions. It is expected that significantly fewer drops will occur in normal usage (e.g.  $< 5$  drops over the lifetime of the device) and generally from a lower height (e.g.  $< 1$  m or table height).

Two devices were tested, with each device dropped a total of 30 times. The drop test protocol comprises a baseline force measurement block ( $M_{PRE}$ ) followed by five repetitions of a drop cycle block ( $D_n$ ) and subsequent force measurement blocks ( $M_n$ ),  $n \in [1, 5]$ , where the measurement accuracy of each GripAble was re-evaluated. Each  $D_n$  consists of six drops from shoulder height of

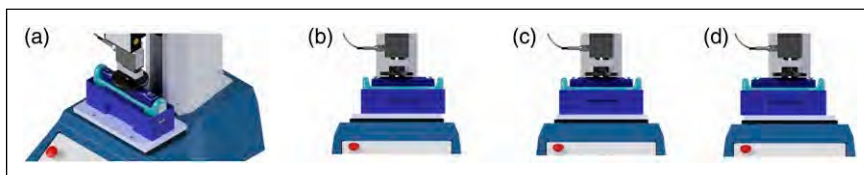


Figure 5. (a) Renderings of the tri-positional test jig. Also showing the (b) bottom, (c) centre, and (d) top positions.

approximately 1.5 m onto a rigid wooden board 50 mm thick in each of the six principal orientations. Each  $M_n$  block follows the same process used for calculating the measurement accuracy against known loads. At the end of the test, both devices were visually inspected for physical damage.

The behaviour of the device freefall during each drop was also analysed from the auxiliary motion sensor data recorded from the GripAble device. Figure 6 summarises the analysis performed. The motion data consists of orientation data as a quaternion (sampled at 50 Hz) and interleaved calibrated accelerometer and raw magnetometer data (each sampled at 25 Hz).

## Results

### Measurement accuracy against known loads

The measurement error across the 47 devices was calculated from the difference between the calibration force and

applied force. Figure 7 shows the individual errors at each force level and for each device as a strip plot, highlighting that error generally increases with force level, especially at the extremities of the device. The elastic force error results show, when the CoP is towards the bottom of the device (Figure 7(a)), there are increasing positive errors as the force is increased. When the CoP is towards the top of the device (Figure 7(c)), the opposite is shown where there are increasing negative errors. In the centre, the errors are spread around zero. For the isometric case, the errors are mostly distributed around zero with a slight negative trend when the CoP is towards the top of the device (Figure 7(f)). This mismatch can be attributed to the fact that the load cells are bending beams (each 38 mm long) themselves configured as per Figure 2. Any deflection of the load cell beams when the CoP is not at the midpoint between the two load cells will cause the beams to deflect different amounts relative to the midpoint, and is not accounted for by the simple linear model employed (Equation (5)).

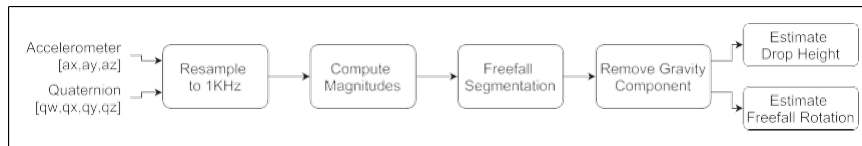


Figure 6. Analysis used to estimate the drop height and freefall rotation based on the motion sensor data recorded during drop cycles.

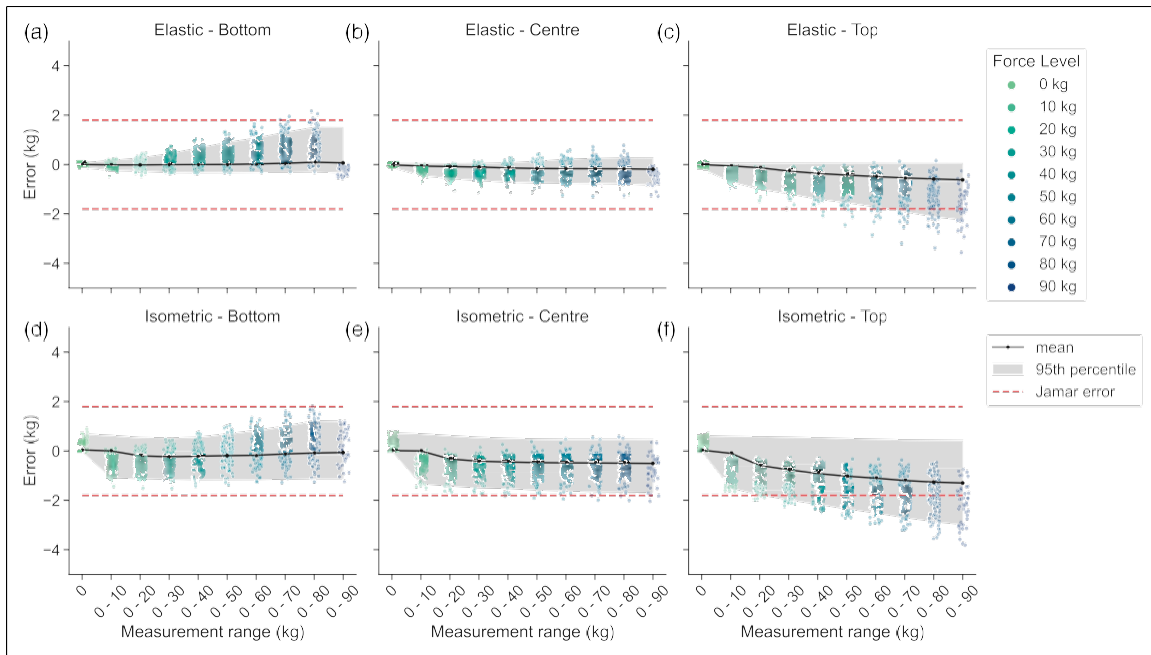


Figure 7. Strip plot showing individual errors at each force level and distribution of error as mean (solid line) and 95<sup>th</sup> percentiles (shaded area) across different measurement ranges. Also shown is the advertised error of Jamar directly following recalibration (dotted line).

Table 2. Hysteresis mean  $\pm$  std % (95<sup>th</sup> percentile) across devices for each position (bottom, centre and top) and mode (elastic, isometric).

Mean $\pm$ std (95 <sup>th</sup> percentiles)	Bottom	Centre	Top
Elastic	0.25 $\pm$ 0.12% (0.11%, 0.59%)	0.32 $\pm$ 0.14% (0.14%, 0.72%)	0.36 $\pm$ 0.20% (0.18%, 0.91%)
Isometric	0.31 $\pm$ 0.12% (0.15%, 0.63%)	0.35 $\pm$ 0.12% (0.19%, 0.63%)	0.35 $\pm$ 0.16% (0.17%, 0.77%)

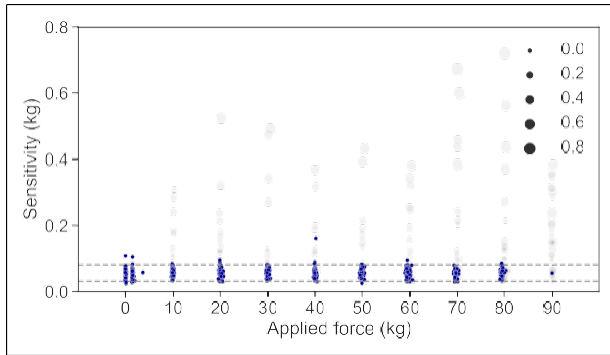


Figure 8. Scatter plot showing measurement sensitivity across the applied force level. The marker size indicates the variability of the applied force based on the peak-to-peak range with  $\Delta F > 0.0$  excluded from the 'static' sensitivity measures. The dotted lines represent the 95<sup>th</sup> percentiles of the measurement sensitivity.

In general, the isometric force errors (Figures 7(d)–(f)) are higher than the elastic force errors (Figures 7(a)–(c)). This may be caused by the influence of the locking mechanism, which may add a small and inconsistent nonlinearity to the start of the isometric force measurement due to a small amount of play ( $< 1$  mm) required by the locking subsystem. Moreover, this play can vary between 0 and 1 mm due to manufacturing tolerances leading to less consistent behaviour. Specifically, at zero force the load cells are blocked by the locking subsystem, with this load transitioning to the hand when force is applied, adding an additional spring reaction force into the measurement. Although minimising this play is desirable for measurement, a small amount is required to ensure the operator can smoothly transition between the elastic and isometric modes.

As grip force is measured in a range and not a single force level, Figure 7 also shows the error distribution for typical force ranges. This was calculated by accumulating the errors at consecutive force intervals starting at zero load, that is, at 0 kg (0 N), 94 data points were used to calculate the measurement range error, while at 0–10 kg (0–98.1 N), 188 data points were used, and at 0–20 kg (0–196.1 N), 282 data points were used, etc. The mean (black line) and 95<sup>th</sup> percentiles (shaded area) across the 47 GripAbles are also shown. For comparison, the errors associated with the industry-standard Jamar are shown as dotted lines and were extracted from a recent calibration certificate provided by

the supplier (2 months prior to testing). These plots indicate that for the centre and bottom positions, the device's accuracy is equal to or better than the Jamar device.

Across the 47 GripAbles tested, the Pearson correlation coefficient revealed that average devices' concurrent validity against known loads was  $0.9997 \pm 0.0002$  (mean  $\pm$  std) and ranged between 0.9991 and 0.9999 (95<sup>th</sup> percentiles).

The hysteresis across all 47 GripAbles was calculated between the loading and unloading cycles, and the results are as shown in Table 2. The overall hysteresis across all devices, positions and modes was  $0.32 \pm 0.15\%$  (mean  $\pm$  std) and ranged between 0.14% and 0.73% (95<sup>th</sup> percentiles).

### Measurement sensitivity

Figure 8 shows the peak-to-peak noise distributions across 47 GripAbles when the finger plate is unloaded and at applied forces up to 90 kg (882.6 N). Some trials exhibited additional signal perturbations at applied forces greater than zero due to the Mecmesin force testing machine's control system. These trials are shown as larger transparent dots but have been excluded from the measurement sensitivity calculation due to the variability in the applied force.

Overall, GripAble's measurement sensitivity was  $62.1 \pm 15.3$  g (mean  $\pm$  std) and ranged between 34.4 g and 89.8 g (95<sup>th</sup> percentiles), independent of the applied force level. The distribution of measurement sensitivity across the static applied force levels is shown in Figure 8.

### Drop robustness

**Grip force accuracy.** Figure 9 shows the stability of measurement accuracy for each position (bottom, centre, top) and mode (elastic, isometric) shown across all measurement blocks ( $M_{PRE}$ ,  $M_{1-5}$ ). The scatterplots show the error for each device and force level with the colour indicating the applied force (0–90 kg; 0–882.6 N) alongside the mean error across force levels for each of the two devices. In general, there was minimal effect from dropping on measurement accuracy across all positions and modes, especially during the elastic force measurement.

Table 3 shows the change in measurement error after 30 drops, measured from both GripAbles. Paired t-tests comparing the final  $M_5$  errors to the  $M_{PRE}$  baseline highlight a small but significant average decrease in the absolute errors at the centre point but increase in the errors

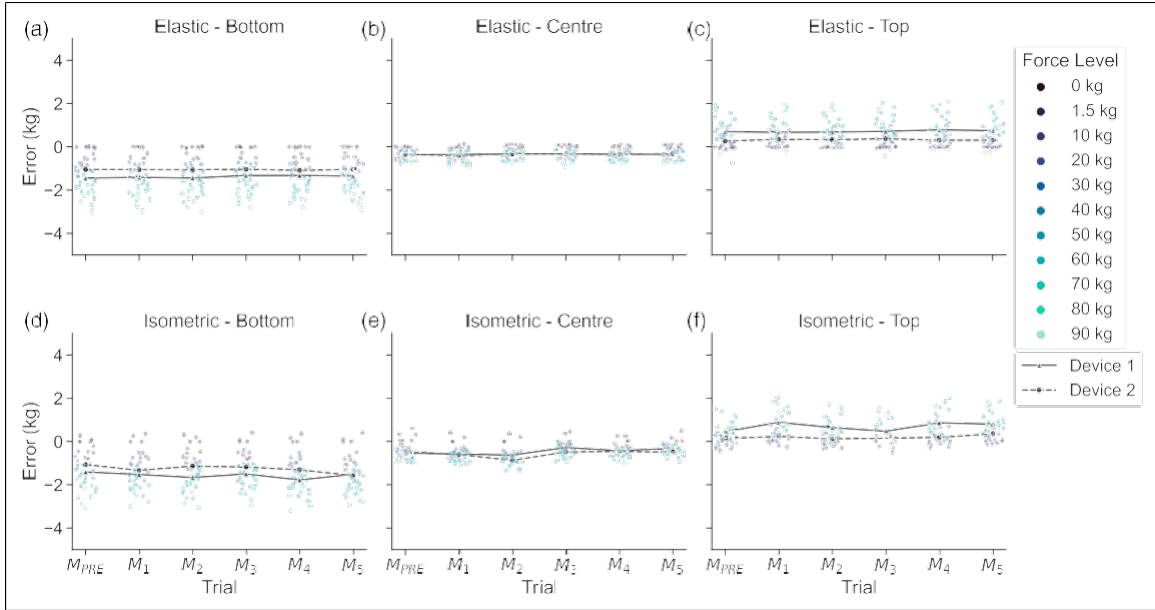


Figure 9. Scatterplot showing the distribution of measurement error following each drop cycle ( $M_{PRE}$ ,  $M_1 - M_5$ ) for two devices. Each subplot represents a different mode (elastic, isometric) and positional (bottom, centre, top) measurement configuration. The mean error across force levels is also shown for each device and trial.

Table 3. Difference in absolute errors ( $M_5 - M_{PRE}$ ), mean  $\pm$  std ( $p$ -value) for each position (bottom, centre and top) and mode (elastic, isometric). The  $p$ -value is from a paired t-test comparing the final  $M_5$  errors to the  $M_{PRE}$  baseline.

Mean $\pm$ std ( $p$ -value)	Bottom	Centre	Top
Elastic	$0.049 \pm 0.239$ ( $p = 0.075$ )	$0.014 \pm 0.251$ ( $p = 0.247$ )	$0.016 \pm 0.231$ ( $p = 0.115$ )
Isometric	$0.232 \pm 0.373$ ( $***p < 0.001$ )	$0.143 \pm 0.300$ ( $**p = 0.001$ )	$0.139 \pm 0.300$ ( $***p < 0.001$ )

at the extremities in isometric mode. There was no significant change for the elastic mode. This may suggest that shock loading caused a small shift in the isometric force baseline due to a perturbation of the mechanical locking subsystem. However, the shift was relatively small on average and is likely to be corrected by the real-time zero drift correction.

No major damage was detected following the 30 drops. However, minor damage, including a small chip in the corner of one of the backplates and scuff marks at the top and bottom of the device were found.

**Drop motion.** Across all 60 drops (combining data from both devices), the drop height was computed as  $1.32 \pm 0.18$  m (mean  $\pm$  std) during freefall (i.e. release-to-impact). This aligns with the devices being dropped from the shoulder height of a 6 ft 3 in tall male, that is, a drop height of approximately  $1.55 \pm 0.1$  m. However, the difference and higher variability in the height estimate can be attributed to inaccuracy due to double integration of the imperfect acceleration values, a relatively low sampling rate (25 Hz) and small segmentation errors when estimating the release and impact timepoints. Unfortunately, the shock loading during impact

could not be accurately computed from the accelerometer data due to the short timescales and the small measurement range of  $\pm 2$  g.

Figure 10 highlights how the device rotated during each trial based on the recorded quaternion data when dropped from each of the six principal orientations. For each subplot, the principal orientation has been aligned with the gravity vector in the direction of the principal axis, that is, pointing downwards towards the floor. The device's rotational trajectories (black dotted lines) are shown, assuming the device is fixed to the sphere and moves relative to the start position (or floor). The red dots indicate the final impact orientation.

When the device is dropped with the  $z$ -axis perpendicular to the gravity vector, its rotation is generally around its  $z$ -axis. The device also tends to orientate onto its side upon impact. This supports what was observed and can be attributed to the device's shape and distribution of the internal mass. Specifically, Figures 10(a) and (d) highlight that when the device is dropped with the finger plate down or up the device rotates approximately  $90^\circ$  in both directions around the  $z$ -axis to land more on its side. When the device is dropped already on its side, that is, Figures 10(b) and (e),

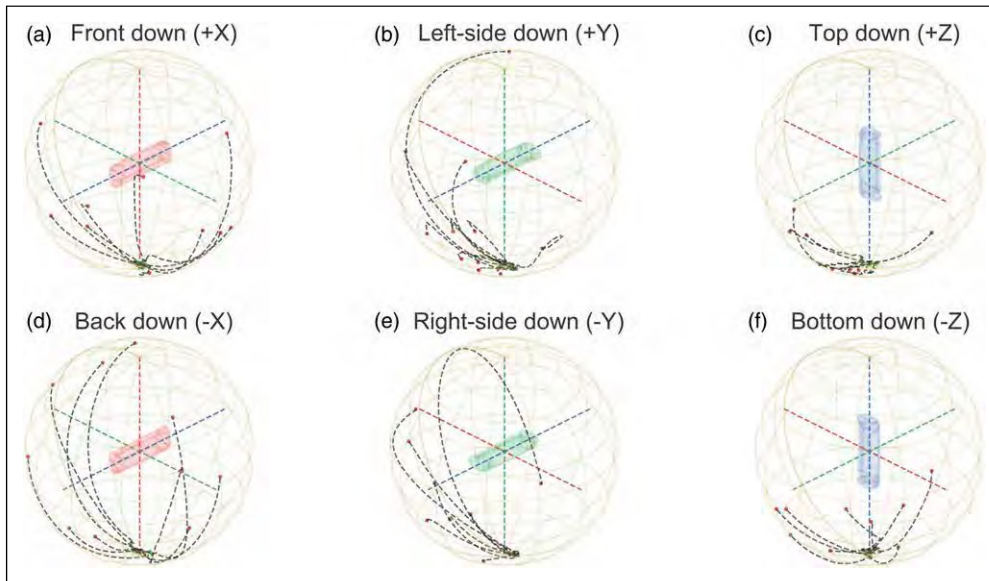


Figure 10. Rotational trajectories of the two devices from release-to-impact for each drop trial. The subplots show the individual trials associated with the six different starting orientations. The starting orientation is shown relative to the floor. The trajectory (dotted line) shows the rotation of the device from the starting vector (south pole) to the point of impact.

there is generally much less rotation and it is in one direction around the  $z$ -axis. However, on occasion, the angular momentum will attempt to orientate the device onto its opposing side (indicated by the larger arc lengths). Conversely, Figures 10(c) and (f) suggest that when the device is dropped with the  $z$ -axis aligned with the gravity vector there is little rotation indicating that the device hits the floor in a similar orientation, that is, upright with a slight tilt.

This analysis highlights that the most likely impact points are on the side, top or bottom of the device, which, by design, provides additional impact protection, as the casework, rather than the force measurement mechanism itself, is absorbing the shock loading caused through repeated dropping.

## Discussion

Results across 47 devices demonstrate that the GripAble device exhibits 1.8 kg – less than 2% full-scale – accuracy. It has low hysteresis at less than 0.73% full scale, suggesting that it remains accurate for measuring both force generation and release, such as in quantitative myotonia assessment, which measures muscle relaxation during maximal contractions.<sup>37</sup>

A small but systematic change in the error relative to loading position was found, leading to overestimation of the force at the bottom of the device and underestimation of the force at the top. This is likely to be caused by the asymmetric configuration of the two short bending beam load cells within the device (each 38 mm long). This error was deemed acceptable as the device will normally be gripped in the central position, especially during standardised grip strength measurement protocols. The measurement mode

(i.e. isometric, elastic) also seems to influence this behaviour. In the future, a more complex, nonlinear model that considers all these factors could potentially be developed to remove this systematic inaccuracy.

A sensitive assessment device is vital for detecting the ‘minimum clinically important difference in grip strength’. Recent studies suggest that grip strength changes of 5.0–6.5 kg may be reasonable estimates of meaningful change,<sup>38</sup> with such change perceived to be beneficial and sufficiently large to warrant an alteration in a patient’s management. A device should also be sensitive enough for detecting grip strength changes in weak individuals, such as post-stroke or post-surgery who can exhibit grip strength below 1 kg. The sensitivity test results show that the GripAble device can sense  $62.1 \pm 15.3$  g changes in force, making it an order of magnitude more sensitive than is required to detect a clinically important change in grip strength, something traditional grip assessment devices fail to do.

The drop test results show that the device is robust to multiple consecutive drops from heights exceeding 1.5 m, with minimal changes in accuracy and little physical damage, suggesting that it can tolerate rough handling without jeopardising performance or accuracy. To the best of our knowledge, the robustness of other grip strength assessment devices, including Jamar, has never been tested, therefore, a direct comparison of GripAble’s performance to existing grip strength assessment devices cannot be made.

GripAble has the flexibility to switch between elastic and isometric. While grip strength is typically assessed isometrically, our previous study found that grip control of novice users improved when training against an elastic load.<sup>30</sup> Results

also highlight that GripAble remains accurate and sensitive in both modes. Therefore, users can use the two modes interchangeably for a more versatile approach to assessment and training of hand function.

GripAble is linked to a custom mobile software platform to provide the benefits of digital and accessible therapy. Such technology supports the recent paradigm shift to a remote care model, driven by COVID-19, which has decimated therapy services and left millions of people requiring rehabilitation untreated.<sup>20–22</sup> For example, users will be able to regularly test their grip strength while allowing therapists to remotely monitor and assess their patients, both accurately and reliably over time, without their physical supervision. Instead, the integrated sensors within the GripAble device and software can facilitate therapists in tracking user compliance to the standard grip strength protocol by analysing hand pose, the time-varying force profile and associated timings of key events, such as rise time, peak force and decay period. Moreover, the software can be used to provide a variety of grip strength measures, including but not limited to, grip endurance, sustained gripping, rapid exchange,<sup>39</sup> gripping rotatory impaction<sup>40</sup> and sine wave grip dexterity tests.<sup>41</sup> Ultimately, these will provide a holistic and objective view of hand function, which is of paramount importance, especially when normal face-to-face observational assessments can no longer be routinely performed.

## Conclusion

This paper has demonstrated GripAble's excellent performance for assessing grip strength due to its accuracy, sensitivity and robustness. Further, bench and in-life tests are required to establish how the device's performance changes over time and for how long the calibration remains valid. Moreover, a direct comparison to the industry-standard Jamar dynamometer regarding measurement robustness and sensitivity is required to validate these claims. An opportunity exists to generate an updated normative grip strength dataset for the modern world, consistent with shifts in culture and epidemiology. GripAble provides a new mobile system enabling the possibility of this information to be collected and centralised at a population scale never achieved, maintaining an evolving digital dataset of regional and international comparisons to be used in healthcare and related research for future generations.

## Acknowledgements

The authors would like to thank Dr. Virgil Mathiowetz for reviewing the manuscript and for his insightful feedback and discussion.

## Declaration of conflicting interests

The author(s) declared the following potential conflicts of interest with respect to the research, authorship, and/or publication of this article: SAM, MO, MM and NG are the employees of GripAble Limited.

## Funding

The author(s) received no financial support for the research, authorship, and/or publication of this article.

## Contributorship

MM and SAM wrote the manuscript. MO and MM developed the calibration system and test setup. MM, SAM, MO and EB designed the protocol for bench tests. MM carried out the bench tests and data analysis. MM and EB are the owners of GripAble's patent and developed the force sensing mechanism. NG advised on the clinical aspects of the manuscript. All authors reviewed and edited the manuscript and approved the final version.

## ORCID iDs

Michael Mace [□ https://orcid.org/0000-0001-9599-448X](https://orcid.org/0000-0001-9599-448X)  
 Sarah Abdul Mutalib [□ https://orcid.org/0000-0003-2226-080X](https://orcid.org/0000-0003-2226-080X)  
 Matjaz Ogrinc [□ https://orcid.org/0000-0001-7944-8083](https://orcid.org/0000-0001-7944-8083)

## References

1. Gale CR, Martyn CN, Cooper C, et al. Grip strength, body composition, and mortality. *Int J Epidemiol* 2007; 36: 228–235.
2. Rantanen T, Harris T, Leveille SG, et al. Muscle strength and body mass index as long-term predictors of mortality in initially healthy men. *J Gerontol Ser A Biol Sci Med Sci* 2000; 55: M168–M173.
3. Ortega FB, Silventoinen K, Tynelius P, et al. Muscular strength in male adolescents and premature death: cohort study of one million participants. *BMJ* 2012; 345: e7279. Epub ahead of print 24 November 2012
4. Wind AE, Takken T, Helder PJM, et al. Is grip strength a predictor for total muscle strength in healthy children, adolescents, and young adults?. *Eur J Pediatr* 2010; 169: 281–287.
5. Reeve TE, Ur R, Craven TE, et al. Grip strength measurement for frailty assessment in patients with vascular disease and associations with comorbidity, cardiac risk, and sarcopenia. *J Vasc Surg* 2018; 67: 1512–1520.
6. Nacul LC, Mudie K, Kingdon CC, et al. Hand grip strength as a clinical biomarker for ME/CFS and disease severity. *Front Neurol* 2018; 9: 992.
7. Roberts HC, Syddall HE, Butchart JW, et al. The association of grip strength with severity and duration of Parkinson's. *Neurorehabil Neural Repair* 2015; 29: 889–896.
8. Leong DP, Teo KK, Rangarajan S, et al. Prognostic value of grip strength: findings from the prospective urban rural epidemiology (PURE) study. *Lancet* 2015; 386: 266–273.
9. Mathiowetz V. Comparison of Rolyan and Jamar dynamometers for measuring grip strength. *Occup Ther Int* 2002; 9: 201–209.
10. Bechtol CO. Grip Test. *J Bone Joint Surg* 1954; 36: 820–832.
11. Mathiowetz V, Kashman N, Volland G, et al. Grip and pinch strength: normative data for adults. *Arch Phys Med Rehabil* 1985; 66: 69–74.

12. Fess EE and Moran C. *Clinical assessment recommendations*. 1st ed. Indianapolis: American Society of Hand Therapists, 1981, [https://www.researchgate.net/publication/303400806\\_American\\_Society\\_of\\_Hand\\_Therapists\\_Clinical\\_Assessment\\_Recommendations](https://www.researchgate.net/publication/303400806_American_Society_of_Hand_Therapists_Clinical_Assessment_Recommendations) (accessed 12 March 2021).
13. MacDermid J, Solomon G, Valdes K, et al. Clinical assessment recommendations. In: *Impairment-based conditions*. 3rd ed. New Jersey: Mount Laurel, N.J.; 2015.
14. Mathiowetz V, Weber K, Volland G, et al. Reliability and validity of grip and pinch strength evaluations. *J Hand Surg* 1984; 9: 222–226.
15. Mathiowetz V, Vizenor L and Melander D. Comparison of baseline instruments to the Jamar dynamometer and the B&L engineering pinch gauge. *Occup Ther J Res* 2000; 20: 147–162.
16. Svens B and Lee H. Intra- and inter-instrument reliability of grip-strength measurements: griptrack and Jamar hand dynamometers. *Br J Hand Ther* 2005; 10: 47–55.
17. Roberts HC, Denison HJ, Martin HJ, et al. A review of the measurement of grip strength in clinical and epidemiological studies: towards a standardised approach. *Age Ageing* 2011; 40: 423–429.
18. Mathiowetz V, Wiemer DM and Federman SM. Grip and pinch strength: norms for 6- to 19-year-olds. *Am J Occup Ther* 1986; 40: 705–711.
19. Fain E and Weatherford C. Comparative study of millennials' (age 20-34 years) grip and lateral pinch with the norms. *J Hand Ther* 2016; 29: 483–488.
20. Ward G and Casterton K. *The impact of the COVID-19 pandemic on occupational therapy in the United Kingdom Survey report*, 2020, [https://www.rcot.co.uk/sites/default/files/The\\_impact\\_of\\_the\\_COVID-19\\_pandemic\\_on\\_occupational\\_therapy\\_in\\_the\\_United\\_Kingdom\\_-\\_Survey\\_report.pdf](https://www.rcot.co.uk/sites/default/files/The_impact_of_the_COVID-19_pandemic_on_occupational_therapy_in_the_United_Kingdom_-_Survey_report.pdf).
21. Prvu Bettger J, Thoumi A, Markevich V, et al. COVID-19: maintaining essential rehabilitation services across the care continuum. *BMJ Glob Health* 2020; 5: 2670.
22. Phillips DM, Turner-Stokes L, Wade D, et al. *Rehabilitation in the wake of Covid-19 -A phoenix from the ashes*, 2020, <https://www.bsrm.org.uk/downloads/covid-19bsrmisue1-published-27-4-2020.pdf>.
23. Fess EE. Guidelines for evaluating assessment instruments. *J Hand Ther* 1995; 8: 144–148.
24. Fess EE. Making a difference: the importance of good assessment tools. *The Br J Hand Ther* 1998; 3: 3.
25. Svantesson U, Norde' M, Svensson S, et al. A comparative study of the Jamar and the grippit for measuring handgrip strength in clinical practice. *Isokinetics Exerc Sci* 2009; 17: 85–91.
26. Hogrel J-Y. Grip strength measured by high precision dynamometry in healthy subjects from 5 to 80 years. *BMC Musculoskelet Disord* 2015; 16, Epub ahead of print 10 June 2015.
27. Gatt I, Smith-Moore S, Steggle C, et al. The takei handheld dynamometer: an effective clinical outcome measure tool for hand and wrist function in boxing. *HAND* 2018; 13: 319–324.
28. Guerra RS, Amaral TF, Sousa AS, et al. Comparison of Jamar and bodygrip dynamometers for handgrip strength measurement. *J Strength Cond Res* 2017; 31: 1931–1940.
29. Rinne P, Mace M, Nakornchai T, et al. Democratizing neurorehabilitation: how accessible are low-cost mobile-gaming technologies for self-rehabilitation of arm disability in stroke? *PLoS One* 2016; 11: e0163413.
30. Mace M, Rinne P, Liardon J-L, et al. Elasticity improves handgrip performance and user experience during visuomotor control. *R Soc Open Sci* 2017; 4: 160961.
31. Mutalib SA, Mace M, Ong HT, et al. Influence of visual-coupling on bimanual coordination in unilateral spastic cerebral palsy. In: IEEE 16th International Conference on Rehabilitation Robotics (ICORR). IEEE, 2019, 1013–1018.
32. Burdet E, Michael AVM, Liardon J-L, et al. *A force measurement mechanism*. ES2744995 (T3). European Patent Office, 2016.
33. International Standards Organisation (ISO). *Calibration and verification of static uniaxial testing machines — Part 1: Tension/compression testing machines — Calibration and verification of the force-measuring system*, 2018. ISO 7500-1:2018, International Standards Organisation (ISO), <https://www.iso.org/standard/72572.html> (accessed 12 March 2021).
34. American Society for Testing and Materials (ASTM). *Standard Practices for Force Verification of Testing Machines*, 2016. ASTM E4-16:2016, American Society for Testing and Materials (ASTM), <https://www.astm.org/Standards/E4.htm> (accessed 12 March 2021).
35. University Loughborough and Aston Business School for the Health and Safety Executive. *RR342 - Revision of body size criteria in standards - Protecting people who work at height*. Health and Safety Executive, 2005, <https://www.hse.gov.uk/research/rrhtm/rr342.htm> (accessed 20 July 2021).
36. Fess EE. A method for checking Jamar dynamometer calibration. *J Hand Ther* 1987; 1: 28–32.
37. Statland JM, Bundy BN, Wang Y, et al. A quantitative measure of handgrip myotonia in non-dystrophic myotonia. *Muscle Nerve* 2012; 46: 482–489.
38. Bohannon RW. Minimal clinically important difference for grip strength: a systematic review. *J Phys Ther Sci* 2019; 31: 75–78.
39. Westbrook AP, Tredgett MW, Davis TRC, et al. The rapid exchange grip strength test and the detection of submaximal grip effort. *J Hand Surg* 2002; 27: 329–333.
40. LaStayo P and Hartzel J. Dynamic versus static grip strength: how grip strength changes when the wrist is moved, and why dynamic grip strength may be a more functional measurement. *J Hand Ther* 1999; 12: 212–218.
41. Rinne P, Hassan M, Fernandes C, et al. Motor dexterity and strength depend upon integrity of the attention-control system. *Proc Natl Acad Sci* 2018; 115: E536–E545.